Plasmonics (2016) 11:11–15
DOI 10.1007/s11468-015-0008-1

Highly Efficient Excitation of Surface Plasmon Polaritons Under Asymmetric Dielectric Surroundings

Yan Guo[1] · **Jianjun Yang**[2] · **Kuanbiao Li**[3]

Received: 26 March 2015 / Accepted: 8 June 2015 / Published online: 3 July 2015

Abstract We demonstrate a single deep subwavelength slit for efficiently improving the excitation of surface plasmon polaritons (SPP) on metals through raising the dielectric permittivity of the output surrounding medium and numerically investigating their physical properties. Via adjusting the slit width and the output permittivity, either SPP launching intensity or its efficiency can be enhanced by almost 25 times and 170 %, respectively, compared with that under the symmetric surroundings. The underlying mechanisms are attributed to the spatial distribution change of the transmitted field and the plasmon density of state (DOS).

Keywords Surface plasmon polaritons · Excitation efficiency · Diffraction · Plasmon density of state

Introduction

The extraordinary optical transmission through the dispersive metallic subwavelength structures has been investigated for several years. It is thought that the surface plasmon polaritons (SPP) play a crucial role in this regime and open a new way in nanophotonics. Therefore, how to elevate or what factors will affect the launching efficiency of SPP is inevitably a very important issue. Recently, many SPP-based metallic nanostructures with different designs have been proposed and studied in both theory [1–5] and experiment [6–9] and attempted to solve this problem. However, these complex structures are usually very hard to fabricate in practice. Even though employing an oblique illumination method can obtain the unidirectional enhancement of SPP intensity [10–12], this is not common in practice. Thus, how to effectively and easily improve the intensity and efficiency of SPP becomes much more needed. On the other hand, the surrounding dielectric medium of subwavelength apertures is also a significant factor to influence the SPP excitation [3, 4], but less attention has been paid to either this parameter or the electromagnetic behavior generated in structures with this parameter, such as interference, which would affect the calculated accuracy.

In this paper, we demonstrate that a further boost of the launching intensity and efficiency of SPP can be achieved by exploiting a single subwavelength metal slit covered by a semi-infinite dielectric medium in the transmission region. On the basis of the finite-difference time-domain (FDTD) simulation, we find some interesting patterns of the transmitted field distribution with varying the slit width and dielectric permittivity ε_d of the output surrounding medium. We propose that the special distribution change of the transmitted field, due to the diffraction generated at the slit exit opening, and the plasmon density of state are the main mechanisms. This structure is simple and easy to produce with high SPP efficiency, which can be widely used for subwavelength optoelectronic devices.

✉ Jianjun Yang
jjyang@nankai.edu.cn

[1] College of Life Information Science and Instrument Engineering, Hangzhou Dianzi University, 310018 Zhejiang, China

[2] Key Laboratory of Optical Information Science and Technology, Education Ministry of China, Institute of Modern Optics, Nankai University, Tianjin 300071, China

[3] HANGZHOU HANGYANG Co. Ltd, Hangzhou 310014, Zhejiang, China

Methodology

A schematic plot of the structure under consideration is sketched in Fig. 1, where a silver thin film is chosen to be the metal material, accompanied with an air slit cut through the film whose width is denoted by w. The substrate of the slit is air, and the semi-infinite coating material above the film is a dielectric medium with permittivity ε_d. A time-harmonic monochromatic Gaussian plane wave normally illuminates the slit from below with the wavelength of λ_0=1 μm, whose magnetic field H_z has the same direction as the slit (transverse-magnetic polarization). The permittivity of silver is described by Drude polarization model with a value of ε_m=−48.8+3.16i at this wavelength [13].

The reason why we do not choose finite thickness of dielectric medium is because the effects on the calculation result are different for different thickness of dielectric medium. For one wavelength thickness of the dielectric medium, as shown in Fig. 2a, the beam transmitted from the slit will be reflected partially back into the dielectric medium at the glass and air interface. According to Fresnel's law, when a light propagates from a optically denser medium into an optically thinner medium with small incident angles, the phases of the reflection and incident wave on the interface are opposite, leading to destructive interference patterns occurring in the dielectric slab, which will make large calculated error. However, if the dielectric medium is very thin, the interference pattern does not occur and will not influence the calculated result, as shown in Fig. 2b. In order to reduce unnecessary errors, we use an infinite thickness of dielectric medium to simulate the electromagnetic field distribution.

Here, we define several parameters: the transmission efficiency T, which is defined as the ratio of the integrated Poynting vector in Y direction over the slit exit opening to that over the entrance opening; the SPP intensity is defined to be the integration of the modular square of the magnetic field

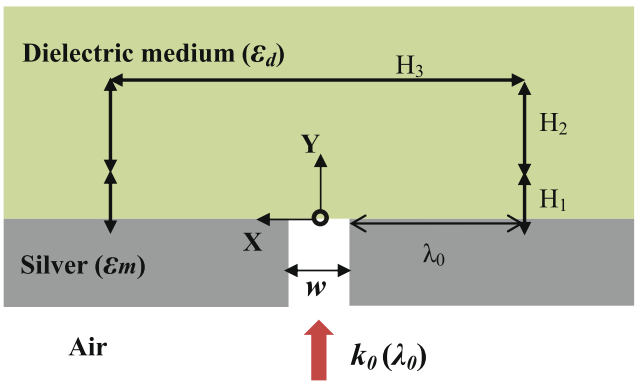

Fig. 1 Schematic plot of a single subwavelength slit structure in silver film associated with air substrate, air-filled slit, and surrounding dielectric medium with permittivity ε_d. A plane wave illuminates the structure in the Y-axis direction from below with the wavelength of λ_0=1 μm. The distances H_1, H_2, and H_3 are taken from Ref. 3

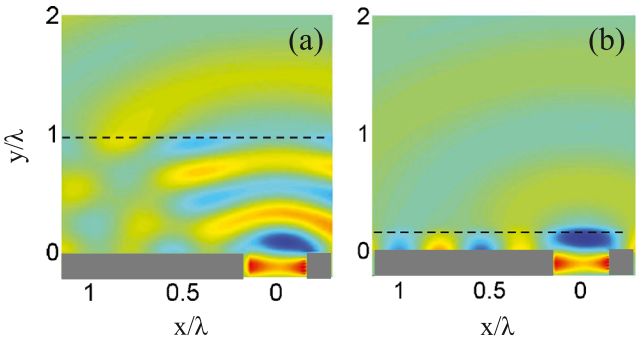

Fig. 2 Simulated magnetic field distribution Hz of Ref. 3 when a glass-filled slit is illuminated by the incident with the wavelength of λ_0= 500 nm, where the slit width is 150 nm, the thicknesses of glass slab placed on the metal are 500 nm (**a**) and 100 nm (**b**), respectively. The dashed lines represent the interfaces of glass and air

along H_1; the SPP launching efficiency η refers to be the ratio of the SPP intensity to the transmitted field total intensity. The integration path of the total intensity is along the double arrow solid lines, including radiative field and SPP.

Results and Discussion

First, we choose several slit widths w from 100 to 400 nm to simulate by using the FDTD method. For each case, the dielectric permittivity of the surrounding medium in the output space is gradually increased, making the whole structure changed from a symmetric surrounding (with the same permittivity above and below the slit) to asymmetric ones (with different permittivities on both sides of the slit). Under each circumstance, the slit width is fixed, but the slit depth is coordinated to satisfy the SPP resonance in the slit so that the maximum energy flux can be obtained at the slit exit opening. Through this adjustment, the influence of the film thickness on the SPP launching cannot be considered again. In simulations, the Y component Poynting vector is integrated respectively over the exit or entrance apertures of the slit, and the calculated transmission efficiencies T are shown in Fig. 3a. It is seen that for each slit width, T at small ε_d remains almost the same values as that under the symmetric surroundings (ε_d=1) and then gradually decreases with the increase of ε_d. In addition, the curve of transmission efficiency begins to shift downward for the broad slit. These results indicate that the electromagnetic energy transmission to the slit exit opening becomes less with increasing both the output permittivity and the slit width. It is in sharp contrast to the traditional idea that much more energy can transmit from larger apertures, especially for the larger output permittivity, in which the slit is not a subwavelength slit any more compared with the wavelength in the output space.

Then, we calculate the SPP intensity through integrating the modular square of the normalized magnetic field from

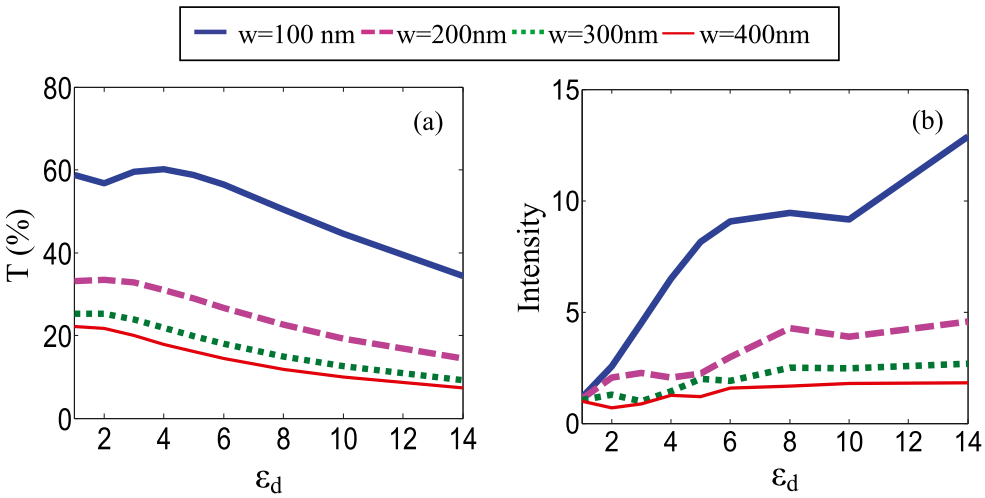

Fig. 3 Calculated transmission efficiency T (**a**) and SPP intensity (**b**) as a function of the dielectric permittivity of the output medium at several slit widths

both transverse sides of the slit, as shown in Fig. 3b. At first glance, each curve presents a rising tendency with lager dielectric permittivities, but with a rising rate inversely proportional to the slit width. For example, the maximum SPP intensity increases more than ten times at w=100 nm, but it is only about one time at w=400 nm. We can conclude that the large intensity of SPP can be achieved with the large output permittivity and the small slit width. More interestingly, the conditions for gaining large SPP intensity correspond to those for getting low transmission efficiencies of the slit. Accordingly, the large SPP intensity is not physically originated from funneling more incident energy into the slit, but supposed to derive from the spatial distribution change of the transmitted light.

For the sake of confirming this assumption, we simulate the magnetic field distributions at different conditions. Figure 4a displays the spatial distribution of H_z field component at ε_d=4 and w=100 nm, wherein the distribution pattern is seen relatively uniform accompanied with a slight increment of the SPP intensity. When the output permittivity is ε_d>4, the SPP

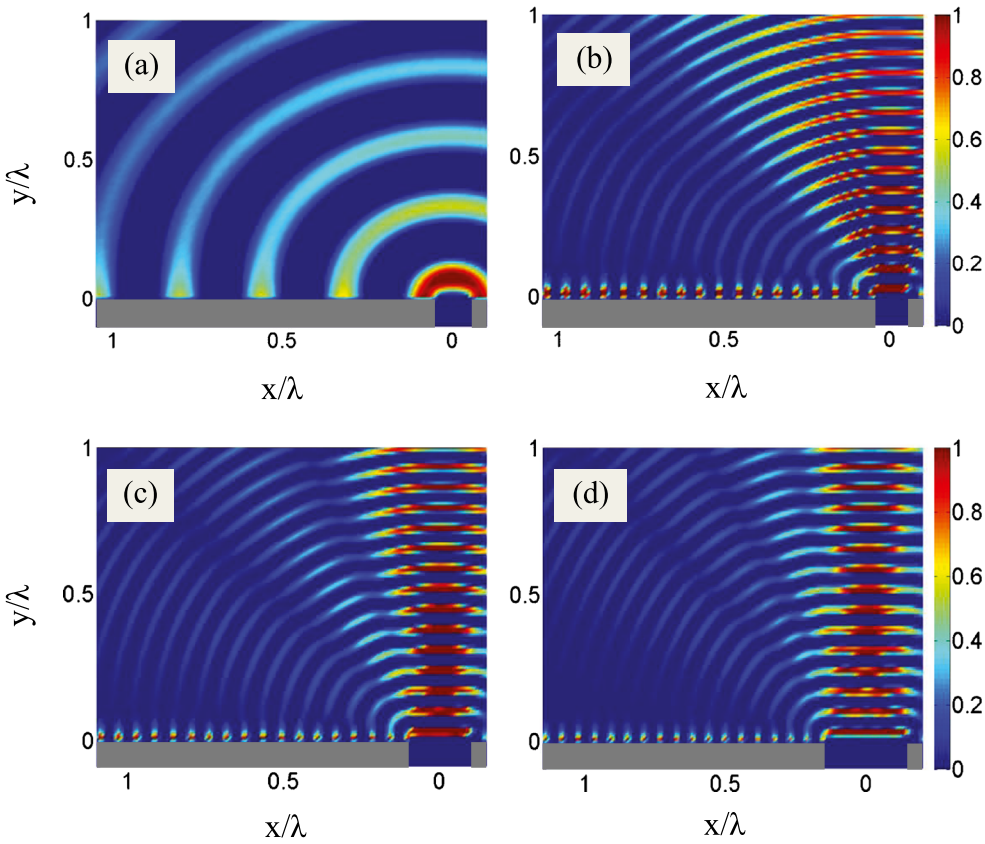

Fig. 4 Simulated near-field distributions of the normalized magnetic field Hz with ε_d=4 (**a**) and ε_d=14 (**b**) at w=100 nm. (**c**) and (**d**) represent the field distributions at w=200 nm and w=300 nm with ε_d=14, respectively. Only the left region of the output space is given due to the symmetric distributions along the central line of the structure. The gray slabs represent the metal film

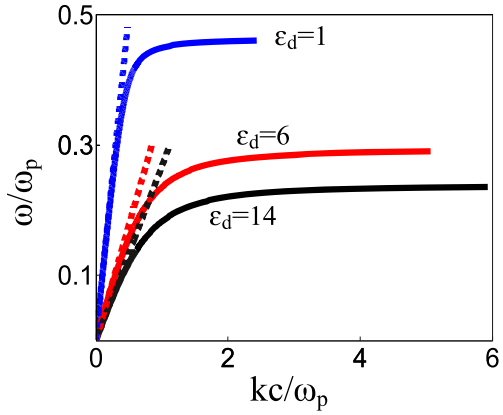

Fig. 5 Dispersion relation of SPP under the surrounding conditions with different dielectric permittivities

intensity is evidently enhanced with a distinct separation from the radiative beam approaching the interface. The spatial separation is originated from the reinforced confinement of SPP caused by the increased ε_d, rather than caused by the reduction of incident wavelength leading to the change of ε_m [14]. When ε_d is increased up to 14, whose field distribution is patterned in Fig. 4b, a new separation of the transmitted beam begins to appear. The intensities of SPP and the radiative beam positioned right above the slit are considerably increased, but the intensity of the beam part between the two separations drops greatly, which is a sharp reminder of a higher order diffraction beam. This phenomenon indicates that the slit acts as a diffraction aperture when ε_d is pretty large, not as a point source any more (ε_d=1) generated uniformly distribution of the transmitted beam [15]. As a result, SPP is confined to locate on the interface, and the zeroth-order transmitted beam (right above the slit) becomes narrower in width and stronger in amplitude, finally leading to the beaming of light [16].

With widening the slit, the diffraction becomes more drastical: The spatial distributions of both the zeroth-order transmitted beam and SPP are compressed even more with enhanced intensities, but the former enhancement is larger than the latter. Figure 4c, d presents the field modifications with the same permittivity of ε_d=14 at w=200 and 300 nm, respectively. We can conclude that the spatial distribution change of the transmitted field accounts for the enhanced intensity.

Furthermore, in virtue of keeping a nearly constant transmission efficiency T (Fig. 3a) when $\varepsilon_d \leq 6$ at w=100 nm, we can confirm that the spatial distribution change of the transmitted beam cannot fully explain the corresponding fast-rising tendency of the SPP intensity (Fig. 3b). Another reason is that the excitation of SPP at the metal interface also improves greatly. This point can be explained by the plasmon density of state (DOS), which is determined by the factor $d(k^2)/d(\hbar\omega)$ [17]. For a given light incidence, DOS has an inverse relationship with the slope of the dispersion curve. With increasing the dielectric permittivity of the output surrounding medium, the slope of the dispersion relation curve drops (seen from Fig. 5), leading to the DOS increase and the corresponding enhanced SPP excitation.

We also calculate the launching efficiency (η) of SPP for further investigating its percentage in the whole transmitted field. The result is shown in Fig. 6a. At the symmetric surrounding condition, η has small declines with the increase of w. When ε_d increases for a given slit width, the variation tendencies are different. In the case of w=100 nm, η first increases to the maximum at ε_d=5 and then drops down slowly until it reaches dip and begins to rebound. For other cases, however, η drops sharply at first and then changes with the growth trend. Meanwhile, the maxima intensity and efficiency are not achieved at the same time. For example, the efficiency reaches the maximum at ε_d=5 for w=100 nm, but the intensity does not achieve its peak under the same condition. We find that the enhanced launching efficiency of SPP with the asymmetric surrounding conditions can be achieved at w=100 nm or even smaller slit widths in comparison with the symmetric one. Moreover, a significant increment of η can be obtained only in a small dynamic range of the output permittivity. In other words, there exists an optimal permittivity for each situation. For w=100 nm, the optimal permittivity is ε_d=5, and its corresponding SPP efficiency can be improved by almost

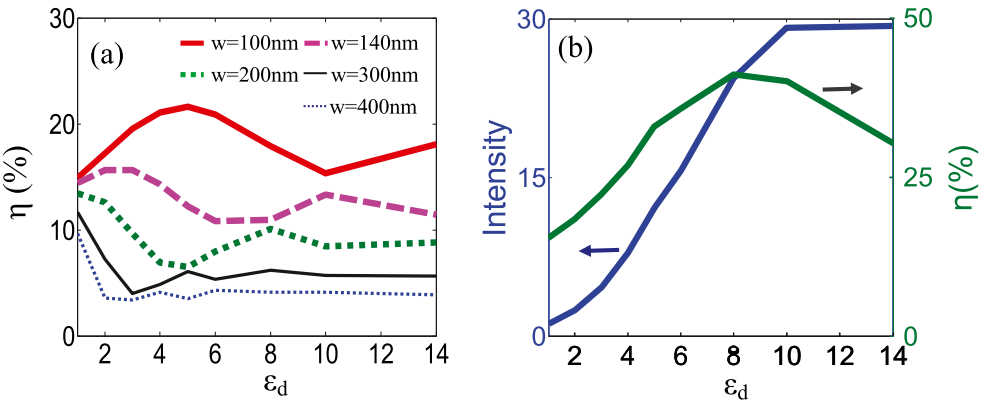

Fig. 6 The launching efficiency of SPP as a function of the output permittivity at different slit widths (**a**). The SPP intensity and its launching efficiency as a function of the output permittivity at w= 60 nm (**b**)

50 %. Therefore, we can predict that the launching SPP efficiency would be further enhanced with narrowing the structure.

In order to prove this prediction, we further make another two simulations, w=140 and 60 nm, whose launching SPP efficiencies are summarized in Fig. 6a, b, respectively. For w=60 nm, the SPP intensity greatly increases to peak at ε_d= 10 and then remains constant, and its launching efficiency is overall enhanced, whose peak is obtained at ε_d=8. Numerically, the SPP intensity and launching efficiency under asymmetric structure are increased 25 times and 170 %, respectively, compared with that under symmetric one, which demonstrates that highly efficient excitation of SPP can be obtained in deep subwavelength structures. Interestingly, the efficiency curves have a quasi-periodic variation with permittivity, whose period increases with decreasing w, and the peak location shifts to small permittivity with increasing w, which may be attributed to the changes of wave vector and initial phase of SPP with the dielectric permittivity and slit width, respectively.

Conclusion

In summary, we have introduced and theoretically investigated a simple and high efficient asymmetric subwavelength structure for improving the intensity and launching efficiency of SPP on the metal surfaces. Simulation results have revealed that the launching SPP intensity can be increased 25 times, and the corresponding launching efficiency η can be elevated up almost 170 % compared with that under the symmetric surrounding. Moreover, such an increment is closely dependent on both the output permittivity and the slit width. Theoretical analysis reveals that both the spatial distribution change of the transmitted field and the DOS are the main mechanisms. Importantly, the peak launching efficiency of SPP does not correspond to its peak intensity. The dielectric permittivity of the output surrounding medium can be flexibly chosen for potential applications in nanoplasmonic devices and bio-sensing.

Acknowledgments This work was supported by the National Science Foundation of China (grant nos. 11304070 and 11274184), the Tianjin National Natural Science Foundation (grant no. 12JCZDJC20200), and the Research Fund for the Doctoral Program of Higher Education of China (grant no. 20120031110032).

References

1. de la Cruz S, Mendez ER, Macias D, Salas-Montiel R, Adam PM (2012) Compact surface structures for the efficient excitation of surface plasmon-polaritons. Phys Status Solidi B 249:1178–1187
2. Lalanne P, Hugonin JP, Rodier JC (2006) Approximate model for surface-plasmon generation at slit apertures. J Opt Soc Am A 23: 1608–1615
3. Mehfuz R, Maqsood MW, Chau KJ (2010) Enhancing the efficiency of slit-coupling to surface-plasmon-polaritons via dispersion engineering. Opt Express 18:18206–18216
4. He MD, Liu JQ, Wang KJ, Wang XJ, Gong ZQ (2012) Efficient directional excitation of surface plasmon polaritons by partial dielectric filling slit structure. Opt Commun 285:4588–4592
5. Ceperley DP, Neureuther AR (2008) Engineering surface plasmon grating couplers through computer simulation. J Vac Sci Technol B 26:2183
6. Baudrion AL, de Leon-Perez F, Mahboub O, Hohenau A, Ditlbacher H, Garcia-Vidal FJ, Dintinger J, Ebbesen TW, Martin-Moreno L, Krenn JR (2008) Coupling efficiency of light to surface plasmon polariton for single subwavelength holes in a gold film. Opt Express 16:3420–3429
7. Mehfuz R, Chowdhury FA, Chau KJ (2012) Imaging slit-coupled surface plasmon polaritons using conventional optical microscopy. Opt Express 20:10526–10537
8. Ferri FA, Rivera VAG, Osorio SPA, Silva OB, Zanatta AR, Borges BHV, Weiner J, Marega E (2011) Influence of film thickness on the optical transmission through subwavelength single slits in metallic thin films. Appl Opt 50:G11–G16
9. Kihm HW, Lee KG, Kim DS, Kang JH, Park QH (2008) Control of surface plasmon generation efficiency by slit-width tuning. Appl Phys Lett 92:051115
10. Sonnerfraud Y, Kerman S, Di Martino G, Lei DY, Maier SA (2012) Directional excitation of surface plasmon polaritons via nanoslits under varied incidence observed using leakage radiation microscopy. Opt Express 20:4893–4902
11. Radko IP, Bozhevolnyi SI, Brucoli G, Martin-Moreno L, Garcia-Vidal FJ, Boltasseva A (2009) Efficient unidirectional ridge excitation of surface plasmons. Opt Express 17:7228–7232
12. Wang J, Chen XS, Lu W (2009) High-efficiency surface plasmon polariton source. J Opt Soc Am B 26:B139–B142
13. Palik ED (1985) Handbook of optical constants of solids. Academic, New York
14. Kihm HW, Kang JH, Kyoung JS, Lee KG, Seo MA, Ahn KJ (2009) Separation of surface plasmon polariton from nonconfined cylindrical wave launched from single slits. Appl Phys Lett 94:141102
15. Guo Y, Zhao B, Yang JJ (2013) Near-field beam focusing by a single bare subwavelength metal slit with the high-index transmission space. Opt Express 21:13949–13957
16. Ebbesen TW, Lezec HJ, Ghaem HF, Thio T, Wolff PA (1998) Extraordinary optical transmission through subwavelength hole arrays. Nature 391:667–669
17. Gontijo I, Boroditsky M, Yablonovitch E, Keller S, Mishra UK, DenBaars SP (1999) Coupling of InGaN quantum-well photoluminescence to silver surface plasmons. Phys Rev B 60: 11564–11567